

Lawrence Berkeley National Laboratory

Recent Work

Title

PSEUDO-QUADRUPOLE COUPLING CONSTANTS AND NUCLEAR MOMENTS OF SEVERAL PROMETHIUM ISOTOPES

Permalink

<https://escholarship.org/uc/item/4f26d3rh>

Authors

Grant, R.W.
Shirley, D.A.

Publication Date

1962-09-01

University of California

**Ernest O. Lawrence
Radiation Laboratory**

TWO-WEEK LOAN COPY

*This is a Library Circulating Copy
which may be borrowed for two weeks.
For a personal retention copy, call
Tech. Info. Division, Ext. 5545*

Berkeley, California

DISCLAIMER

This document was prepared as an account of work sponsored by the United States Government. While this document is believed to contain correct information, neither the United States Government nor any agency thereof, nor the Regents of the University of California, nor any of their employees, makes any warranty, express or implied, or assumes any legal responsibility for the accuracy, completeness, or usefulness of any information, apparatus, product, or process disclosed, or represents that its use would not infringe privately owned rights. Reference herein to any specific commercial product, process, or service by its trade name, trademark, manufacturer, or otherwise, does not necessarily constitute or imply its endorsement, recommendation, or favoring by the United States Government or any agency thereof, or the Regents of the University of California. The views and opinions of authors expressed herein do not necessarily state or reflect those of the United States Government or any agency thereof or the Regents of the University of California.

Sub. for pub. in Phys. Rev.

UNIVERSITY OF CALIFORNIA
Lawrence Radiation Laboratory
Berkeley, California
Contract No. W-7405-eng-48

PSEUDO-QUADRUPOLE COUPLING CONSTANTS AND NUCLEAR
MOMENTS OF SEVERAL PROMETHIUM ISOTOPES

R. W. Grant and D. A. Shirley

September 1962

PSEUDO-QUADRUPOLE COUPLING CONSTANTS AND NUCLEAR
MOMENTS OF SEVERAL PROMETHIUM ISOTOPES

R. W. Grant and D. A. Shirley

Lawrence Radiation Laboratory and Department of Chemistry
University of California
Berkeley, California

September, 1962

ABSTRACT

Nuclei of several isotopes of promethium were aligned at low temperatures by a pseudo-quadrupole interaction in cerium magnesium nitrate and by a magnetic hfs interaction in neodymium ethylsulfate. Pseudo-quadrupole coupling constants were determined for Pm^{143} , Pm^{144} , and 5.4 day Pm^{148} . Nuclear moments were derived for Pm^{143} , 5.4-d Pm^{148} , 41-d Pm^{148} , and Pm^{149} . The spins of 5.4-d and 41-d Pm^{148} were found to be 1 and 6 respectively. Evidence was obtained for spin assignments of 6 to states in Sm^{148} at 1.90, 2.09, and 2.19 MeV. Measurements on Pm^{144} tend to confirm the validity of the temperature scale for cerium magnesium nitrate.

PSEUDO-QUADRUPOLE COUPLING CONSTANTS AND NUCLEAR
MOMENTS OF SEVERAL PROMETHIUM ISOTOPES

R. W. Grant and D. A. Shirley

Lawrence Radiation Laboratory and Department of Chemistry
University of California
Berkeley, California

September, 1962

I. INTRODUCTION

The method of low-temperature nuclear orientation has been used with considerable success in recent years for elucidating certain basic features of nuclear decay processes.^{1,2} Like other experimental techniques, it is most fruitfully employed where it can yield information either uniquely or with greater ease or reliability than can other methods. Thus another area in which nuclear orientation can be particularly useful is in studying certain subtle aspects of internal fields in solids, for example magnetic hyperfine structure in metals.^{3,4} An additional example in this area is the detection of small quadrupole⁵ and pseudo-quadrupole⁶ effects in ionic crystals. In this paper such effects are reported for several promethium isotopes in a lattice of cerium magnesium nitrate (CMN). The pseudo-quadrupole interaction is discussed in terms of crystal field theory. Coupling constants and nuclear moments are derived from the experimental data. The Pm isotopes were aligned in both CMN and neodymium ethylsulfate (NES), and several nuclear parameters of these isotopes and their daughters are also reported.

II. EXPERIMENTAL PROCEDURE

Earlier experiments have shown that Pm isotopes can be aligned in both NES and CMN lattices.^{6,7,8} In the present series of experiments we have aligned (5.4 day) Pm¹⁴⁸ and (41 day) Pm¹⁴⁸ in the NES lattice and Pm¹⁴³, Pm¹⁴⁴, and (5.4 day) Pm¹⁴⁸ in the CMN lattice.

Pm¹⁴³ and Pm¹⁴⁴ were prepared as discussed in ref. 7 and 8 respectively. The Pm¹⁴⁸ isomers were made with roughly equal yield in the Berkeley 60" cyclotron by a (p,n) reaction on Nd¹⁴⁸ (in enriched Nd₂O₃). The target material was passed through a cation-exchange column to separate Pm⁺³ from Nd⁺³. The promethium isotopes were then taken up in saturated solutions of NES or CMN and single crystals, weighing about 5 gm., of the corresponding salts were grown with Pm⁺³ incorporated substitutionally into the Nd⁺³ and Ce⁺³ lattice sites. The crystals were then mounted in an adiabatic demagnetization cryostat described elsewhere.⁹ The temperature range covered in NES was $0.02 < T < 1^{\circ}$ K and in CMN was $0.003 < T < 1^{\circ}$ K. The magnetic temperatures of the salts were measured with coils and an AC mutual inductance bridge¹⁰ and the temperatures were converted to thermodynamic temperatures using the data of Meyer¹¹ for NES and the data of Daniels and Robinson¹² for CMN. The crystals were sufficiently isolated thermally to stay below the helium bath temperature for about 2 hours after each demagnetization. Counting, using multichannel analyzers, was done for a period of from 2 to 5 minutes immediately after each demagnetization. The crystal was then warmed to the helium bath temperature and a normalization count was taken. Appropriate corrections, amounting to about 10% of the anisotropic component of angular distribution, were made for such effects as the finite solid angles subtended by the counters.

III. EXPERIMENTAL RESULTS

A. ^{144}Pm

The decay scheme of ^{144}Pm after Ofer¹³ and Funk, et al.¹⁴ is shown in Fig. 1. From earlier alignment experiments on ^{144}Pm in NES⁸ magnetic hyperfine structure constants, A , for spins of 5 and 6 were available. We have aligned ^{144}Pm in CMN and observed the anisotropies for the 474, 615 and 695 keV γ -rays. The intensity of γ -radiation emitted from oriented nuclei, as defined in the usual way¹⁵, is given as

$$I(\theta) = \sum_k B_k U_k F_k P_k(\cos \theta). \quad (1)$$

For low degrees of alignment this equation can be approximated by

$$I(\theta) = 1 + B_2 U_2 F_2 P_2(\cos \theta) \quad (2)$$

where the higher order terms are negligible. The temperature dependence of $I(\theta)$ for the 695 keV γ -ray at $\theta = 0^\circ$ and $\theta = 90^\circ$ is shown in Fig. 2. The angular dependence of $I(\theta)$ for the 615 keV γ -ray at 0.0031^o K is shown in Fig. 3. The data for this temperature may be fitted by a curve of the form

$$I(\theta) = (+ 0.143 \pm 0.004) P_2(\cos \theta) - (0.003 \pm 0.004) P_4(\cos \theta) \quad (3)$$

The values of $I(0)$ at $T = 0.0031^\circ$ K are given in Table I for the three γ -rays observed. These values show that $U_2 F_2$ of the 474 keV γ -ray is considerably ($24 \pm 7\%$) less than $U_2 F_2$ for the other two γ -rays. The same effect was observed previously in NES.⁸

For "stretched" transitions of the type I (L) I-L (L) I-2L etc., the U_k^F products, hence the angular distributions, should be identical for all γ -rays (i.e., $U_k^F(\gamma_i) = U_k^F(\gamma_{i+1})$, etc.). This can easily be shown by writing out the U_k and F_k functions explicitly in terms of 6-j symbols.¹⁵

The three 6-j symbols that are necessary to the proof all have the form

$$\left. \begin{array}{ccc} j_1 & j_2 & l_1 + l_2 \\ l_1 & l_2 & l_3 \end{array} \right\} . \text{ A one-term expression for 6-j symbols of this form}$$

is given in Edmonds' book¹⁶, and the proof reduces to a few lines of algebra.

It is valid for all I, k, and L. Alternatively the same result may be derived from a similar result of angular correlation theory¹⁷ simply by substituting B_k , the orientation parameter, for F_k^F , the F coefficient for the first γ -ray in a "stretched" cascade.

The fact that the 615 and 695 keV γ -rays are stretched transitions explains why their U_2^F 's are equal. However if the spin of Pm^{144} were 6 and if the E.C. decays also involved only the minimum angular momentum change, the U_2^F of the 474 keV γ -ray should also be the same as that of the succeeding transitions, and this is contrary to the experimental observation.

If one assumes that the spin of Pm^{144} is 6 and that both E.C. decays are of the type $L = 2$, this would lead to a 13% relative reduction in U_2^F (474 keV). If one assumes that the spin of Pm^{144} is 5 and that the 45% branch of the E.C. decay is $L = 2$ and the 55% branch is $L = 1$ this would lead to a 15% relative reduction in U_2^F (474 keV). Ofer¹³ estimated the log ft of the 45% branch to be 8.0 and the log ft of the 55% branch to be 6.8. Thus the above assumption of a higher L for the E.C. of the 45% branch does not seem very reasonable. Another possible explanation for the decrease in U_2^F (474 keV) could be that the lifetime of the 1.784 MeV state was somewhat

longer than that of the 1.310 MeV and 0.695 MeV states. This longer lifetime could permit some degree of reorientation and a subsequent attenuation in the size of the effect. In any case the smaller size of U_2F_2 (474 keV) is not well understood.

B. Pm^{143}

Pm^{143} has been previously aligned in NES.⁷ The decay schemes proposed by Ofer¹³ for Pm^{143} and by Starfelt and Cederlund¹⁸ for Pr^{143} are shown in Fig. 4. We have aligned Pm^{143} in CMN and observed the anisotropy of the 740 keV γ -ray. The temperature dependence of $I(0)$ for this γ -ray is shown in Fig. 5. From this curve it is evident that a very high degree of alignment has been achieved because at the lower temperatures the curve is asymptotically approaching a limit. The angular distribution at $T = 0.0031^\circ K$ could be fitted by the theoretical curve $I(\theta) = 1 + 0.090 \times P_2(\cos \theta)$ to within experimental error, again showing that the terms with $k > 2$ in Eq. 1 were negligible.

The ground state spin of Nd^{143} has been measured as $7/2$ by Murakawa and Ross.¹⁹ This corresponds to an odd parity $f_{7/2}$ state according to shell model theory. Ofer found the 740 keV γ -ray to be predominately M1, implying that the spin of the 740 keV state in Nd^{143} must be $5/2^-$, $7/2^-$ or $9/2^-$. All of these spins are consistent with the data shown in Fig. 5. The shell model predicts that the unpaired 61st proton of Pm^{143} will occupy either a $d_{5/2}$ or $g_{7/2}$ state. By comparing the data in Fig. 5 with the theoretical values of B_2 we can obtain U_2F_2 for the 740 keV γ -ray. If we assume that the spin of Pm^{143} is $5/2$ we obtain $U_2F_2 = -0.093 \pm 0.005$; for a spin of $7/2$ we obtain $U_2F_2 = -0.094 \pm 0.004$.

Bl. Pr¹⁴³

In connection with our work on Pm¹⁴³ we searched for a 740 keV γ -ray associated with the decay of Pr¹⁴³. Starfelt and Cederlund¹⁸ found that the ground state of Pr¹⁴³ lies 922 keV above the ground state of Nd¹⁴³. It might therefore be expected that Pr¹⁴³ would decay to the 740 keV state in Nd¹⁴³. We obtained 10 mc of Pr¹⁴³ (from the Oak Ridge Radioisotopes Division). The Pr⁺³ was subsequently purified on an ion exchange column and any short-lived Pr activities were allowed to decay away for a few days. The half-life we observed for Pr¹⁴³ was 13.5 ± 0.6 days which agrees well with earlier determinations.

The Pr¹⁴³ source was placed between Be absorbers to stop the β -rays and cut down on the production of bremsstrahlung. The photon spectrum observed with a NaI counter was linear out to about 770 keV on a semi-log scale (Fig. 6). A straight line was fitted through the data and then subtracted from the data to get the quantity Δ shown in Fig. 7. The solid curve in Fig. 7 represents the curve we feel best fits the data. The broken line corresponds to a theoretical curve which should be observed if 1.5×10^{-4} % of the Pr¹⁴³ decays produced 740 keV γ -rays. We feel that this curve represents a reasonable upper limit for the γ -transition, yielding $\log ft \geq 11.0$ for the β^- decay which populates this state. This beta branch thus probably involves at least two units of angular momentum carried away by the leptons. Budick et al.²⁰ have recently measured the spin of Pr¹⁴³ as 7/2. Since the 740 keV state of Nd¹⁴³ must have spin and parity 5/2-, 7/2- or 9/2- by virtue of the M1 transition to the 7/2- ground state, the (thus ordinary first-forbidden) beta branch to the 740 keV state from Pr¹⁴³ is incredibly hindered. The $\log ft$ of 11.0 would be high even for a unique first-forbidden transition (which this would be if the spins involved were 5/2+ and 9/2- in

Pr¹⁴³ and Nd¹⁴³). For a nonunique transition this log ft is remarkably high and suggests a new selection rule for β^- decay in this region. A similar example²¹ is furnished by the decay of Nd¹⁴⁷. A statement of this rule which fits the existing data is that the interactions of tensor rank 1 are forbidden, at least for $\Delta I \neq 0$.

C. (5.4 day) Pm¹⁴⁸

The 5.4 day isomer of Pm¹⁴⁸ was aligned in both NES and CMN. The decay schemes of the Pm¹⁴⁸ isomers have been thoroughly investigated recently.²²⁻²⁴ The decay scheme after Reich, et al.²⁴ is given for reference in Fig. 8. The only γ -ray anisotropy we were able to measure accurately was that of the 1460 keV γ -ray. The 910 and 550 keV γ -rays had too much background under them from the 41 day isomer to enable any accurate determination of their anisotropies. The temperature dependence of $I(0)$ for the 1460 keV γ -ray in CMN is shown in Fig. 9.

Reich et al.²⁴ were able to show that the spin of the 1460 keV state in Sm¹⁴⁸ is 1. Based on this result and the data in Fig. 9 we can establish the spin of (5.4 day) Pm¹⁴⁸ as 1-. For the decay of (5.4 day) Pm¹⁴⁸ to the 1460 keV state our data fit either a $1 \rightarrow 1$ or $2 \rightarrow 2$ transition very well but not a $2 \rightarrow 1$ spin sequence. In order to obtain a large enough U_2 with the right sign for a $2 \rightarrow 1$ spin sequence one would have to assume almost pure $L = 2$ for the β^- decay to the 1460 keV state and even in this rather unlikely case (log ft is only 7.8) a small deviation from linearity in $I(T)$ should be observed as indicated by the dashed curve in Fig. 9. The 1- ground state spin assignment for Pm¹⁴⁸ also fixes the spins of the 75 and 135 keV states in Pm¹⁴⁸ as 2- and 6- respectively.²⁴

The temperature dependence of $I(0)$ for the 1460 keV γ -ray in NES is

shown in Fig. 10. In both NES and CMN, $I(\theta)$ was found to fit a $P_2(\cos \theta)$ distribution, showing that terms of higher order than $B_2 U_2 F_2$ were negligible. The 1460 keV transition must be pure dipole, requiring an F_2 of + 0.707. The parameter B_2 must be negative in CMN (see Sec. IV); therefore U_2 must also be negative. The β^- decay which populates the 1460 keV state must be predominantly $L = 1$ since $L = 0$ and $L = 2$ give positive contributions to U_2 . The CMN data establish $U_2 F_2 < -0.23$. Thus U_2 for this γ -ray is less than - 0.33; and the 1.1 MeV β^- branch must be more than 72% of the $L = 1$ type.

We obtained a very rough value of $+0.01 \pm 0.02$ for $B_2 U_2 F_2$ of the 910 keV γ -ray at 0.0033°K in CMN. Thus δ , the E2/M1 amplitude mixing ratio, is -0.06 ± 0.06 . From the angular correlation data,²⁴ δ is determined as $\delta = +0.046 \pm 0.001$. Inasmuch as the sign of δ must necessarily be different between the two experiments^{21,25,26} these results are in good agreement.

D. (41 day) Pm¹⁴⁸

The 41 day isomer of Pm¹⁴⁸ was aligned only in NES. The decay scheme for this isomer is also given in Fig. 8. We were able to observe the anisotropies of the 550, 627, 723, 913 and 1011 keV γ -rays. All the $I(\theta)$ for these five γ -rays showed a pure $P_2(\cos \theta)$ behavior. The temperature dependence of $I(0)$ for the 550 keV γ -ray is shown in Fig. 11. The temperature dependence of $I(\theta)$ for the other γ -rays which we observed had the same form. The parameter $I(0)$ for the five γ -rays at $T = 0.02^\circ \text{K}$ is given in Table II. From this table it can again be seen that $I(0)$ for the 550 and 627 keV γ -rays is the same to within experimental error since these are stretched transitions. We were able to establish limits on B_2 at 0.02°K of $B_2 = 0.26 \pm 0.03$ by computing maximum and minimum values of

U_2 and F_2 for all five γ -rays which were consistent with the decay scheme, which then gave the range of allowed values for B_2 . Since B_2 must be the same for all the transitions at any given temperature the overlap of these values was used to establish the above limits. Now we may combine our data with the angular correlation data²⁴ to establish the spins of the 1.90, 2.09 and 2.19 MeV states of Sm^{148} . The Reich et. al. data are consistent with spins 4 and 6 for the 1.90-MeV state. If the spin of this state were 4, B_2 would have to be 0.17 ± 0.01 at 0.02°K to agree with these data; therefore this spin possibility is ruled out. For a spin assignment of 6, B_2 at 0.02°K would have to be 0.25 ± 0.04 which agrees very well with our value of B_2 and establishes the spin of the 1.90 MeV state as 6.

For the 2.09 MeV state, the angular correlation data are consistent with spins 5 and 6. If the spin of the 2.09-MeV state were 5, B_2 at 0.02°K would have to be 0.19 ± 0.03 to agree with this data and this makes the agreement with our value rather poor. For a spin 6 state, B_2 would have to be 0.27 ± 0.04 which agrees well with our value of B_2 and makes 6 the most likely spin assignment for this state.

The 2.19 MeV state must have spins 4 or 6 to be consistent with the angular correlation data. If the spin of this state were 4, B_2 would have to be 0.20 ± 0.01 at 0.02°K which again is not consistent with our value. A spin assignment of 6 for this state leads to a value for B_2 of 0.28 ± 0.04 , in good agreement with our value. Thus the spin of this state is 6.

It thus seems likely that the spins of the 1.90, 2.09 and 2.19 MeV states are all 6 and that the 723, 913 and 1011 keV γ -rays are all pure E2 transitions.

IV. HYPERFINE STRUCTURE CONSTANTS

The observables in nuclear orientation experiments are complicated functions of the interesting parameters.¹⁵ In all but the simplest case these functions are not easily inverted. Certain assumptions, usually about the multipolarities of unseen transitions, must often be made in using the data to derive such quantities as nuclear moments. As future experimental tests of these assumptions may make the nuclear orientation work subject to re-interpretation, it is desirable to state clearly the assumptions made in interpreting the data. Thus in this section the derivation of coupling constants is discussed.

First the form of the Hamiltonian for Pm^{143} in both the NES and CMN crystals requires separate discussion. Shirley et al.⁸ showed that for Pm^{144} aligned in NES the most important term leading to alignment was the magnetic hyperfine interaction

$$\mathcal{H} = A S_z I_z \quad (4)$$

This interaction produces equally spaced nuclear magnetic substates and as a consequence the leading term in B_2 goes as T^{-2} . We observed this same initial behavior of B_2 in (5.4 day) Pm^{148} (Fig. 10) and (41 day) Pm^{148} (Fig. 11).

Chapman, et al.⁶ showed that for Pm^{149} aligned in CMN the interaction has the quadrupolar form

$$\mathcal{H} = P'' [I_z^2 - (1/3) I(I+1)] \quad (5)$$

This was shown from both the sign and temperature dependence of the γ -ray anisotropy. A quadrupolar interaction produces splittings in the nuclear

magnetic substates which are proportional to I_z^2 and consequently the leading term in the temperature dependence of B_2 is T^{-1} . Our results for Pm^{143} , Pm^{144} , and (5.4 day) Pm^{148} aligned in CMN are in complete agreement with Chapman's observation. In each case the sign of the γ -ray anisotropy in CMN is opposite to that in NES. Further, the temperature dependence of the anisotropy in each case is very accurately represented by an interaction of the quadrupolar form (Figs. 2, 5, and 9). This is especially obvious for Pm^{144} and (5.4 day) Pm^{148} in which the characteristic T^{-1} dependence of $I(\theta)$ is exhibited over the entire attainable temperature range.

Thus it is certainly justifiable to derive an experimental hfs coupling constant, A , from the alignment data in NES and a "quadrupole" coupling constant, P , from the alignment data in CMN. The hfs coupling constants, A , were evaluated in a straightforward manner for (5.4 day) Pm^{148} and (41 day) Pm^{148} in NES and are given in Table III.

For Pm^{+3} in CMN a pseudo-quadrupole interaction is expected (Sec. V). The pseudo-quadrupole interaction is an old problem in atomic spectroscopy (see for example ref. 27). The quadrupole coupling constant, P , and the pseudo-quadrupole coupling constant, P' , are not related in a known fundamental way; they are given by

$$P = C \frac{Q}{4I(2I+1)}, \quad (6)$$

which describes an electric effect, and

$$P' = C' \frac{\mu^2}{I^2} \quad (7)$$

which describes a magnetic effect. The constants C and C' are independent of nuclear parameters and thus have the same values for all Pm isotopes.

For the present axially-symmetric problem, however, the two coupling constants are indistinguishable and only their sum P'' is measurable. Thus the hfs portion of the ground-state spin-Hamiltonian for Pm^{+3} in CMN is

$$\mathcal{H} = (P + P') [I_z^2 - (1/3) I(I + 1)] \equiv P'' [I_z^2 - (1/3) I(I + 1)] \quad (8)$$

We shall refer to P'' as the total quadrupole coupling constant. From our data on Pm^{143} , Pm^{144} and (5.4 day) Pm^{148} in CMN we can evaluate the experimental total quadrupole coupling constants P'' and these are given in Table III.

V. CRYSTAL FIELD THEORY

In order to derive nuclear moments from our alignment data in CMN it becomes necessary to evaluate C' experimentally. This may be done only if the relative sizes of P and P' are known. To estimate these magnitudes we used the crystal field theory of Elliott and Stevens,²⁸ extended by Judd²⁹ to CMN, to work out the eigenvalues and eigenstates for the ground-state manifold of Pm^{+3} in CMN.

The crystal field parameters are found experimentally to change quite smoothly through the rare-earth series and the following set of parameters for Pm^{+3} was obtained by interpolation from the values given by Judd.²⁹

$$A_6^0 \langle r^6 \rangle = -40 \text{ cm}^{-1}, \quad A_6^3 \langle r^6 \rangle = \pm 1850 \text{ cm}^{-1}, \quad A_6^6 \langle r^6 \rangle = 700 \text{ cm}^{-1},$$

$$A_2^0 \langle r^2 \rangle = -40 \text{ cm}^{-1}, \quad A_4^0 \langle r^4 \rangle = -30 \text{ cm}^{-1}, \quad \text{and} \quad A_4^3 \langle r^4 \rangle = \mp 400 \text{ cm}^{-1}.$$

The signs of $A_6^3 \langle r^6 \rangle$ and $A_4^3 \langle r^4 \rangle$ are arbitrary but must be different. Energy matrix elements were evaluated for the 9 states of the lowest level, 5I_4 . The 9×9 matrix reduces to three 3×3 matrices, and the eigenvalue problem involves only solving cubic equations. The eigenvalues and eigenvectors are given in Table IV.

The lowest energy state is a singlet which lies about 19 cm^{-1} below the next (doublet) state. We may now determine the relative sizes of P and P'.

Evaluating P' from³⁰

$$H = \frac{4\beta^2 \beta_N^2 \mu_N^2}{I^2} \langle r^{-3} \rangle^2 (\vec{N} \cdot \vec{I})^2 \quad (9)$$

and using³¹ $\langle r^{-3} \rangle = 36.6 \text{ \AA}^{-3}$ for Pm^{+3} , we obtain

$$P' = 1.48 \times 10^{-3} \frac{g_N^2}{\Delta E} \text{ cm}^{-1} \quad (10)$$

where ΔE is the splitting in cm^{-1} between the ground state singlet and the lowest doublet. For a splitting of 18.8 cm^{-1} , we find

$$P' = 8.39 \times 10^{-5} g_N^2 \text{ cm}^{-1} \quad (11)$$

We can also evaluate the effect of direct coupling between the crystalline field and Q the nuclear quadrupole moment:³⁰

$$P_1 = \frac{3A_2^0 Q}{I(2I-1)} \quad (12)$$

Now to evaluate this quantity we must know $\langle r^2 \rangle$ since only $A_2^0 \langle r^2 \rangle = -40 \text{ cm}^{-1}$ is known. To evaluate $\langle r^2 \rangle$ we used Ridley's Hartree radial wave functions³² which are available for Pr^{+3} and Tm^{+3} . We graphically integrated and obtained $\langle r^2 \rangle = 1.445 \text{ a.u.}$ for Pr^{+3} and $\langle r^2 \rangle = 0.7505 \text{ a.u.}$ for Tm^{+3} . By interpolation we obtained $\langle r^2 \rangle = 1.31 \text{ a.u.}$ for Pm^{+3} . Using this value we calculated

$$P_1 = - \frac{3.28 \times 10^{-6} Q}{I(2I-1)} \text{ cm}^{-1} \quad (13)$$

We next considered the interaction of the 4f electrons with the quadrupole moment.

This can be approximated as²⁸

$$P_2 \approx -\frac{9 e^2 Q}{4I (2I - 1)} \langle r^{-3} \rangle \langle J || \alpha || J \rangle \langle + | J_z^2 - (1/3) J(J+1) | + \rangle \quad (14)$$

Evaluating this term for Pm^{+3} we obtain

$$P_2 \approx + \frac{7.49 \times 10^{-4} Q}{I (2I - 1)} \text{ cm}^{-1} \quad (15)$$

Since all the other states in the lowest level (5I_4) lie considerably higher in energy and the first excited level (5I_5) is about 1586 cm^{-1} higher in energy,³³ perturbations due to higher states may be neglected by comparison. Using a spin of 6 and the magnetic moment of 1.75 n.m. for Pm^{+3} ,¹⁴⁴ we calculate $P = 1.13 \times 10^{-5} Q \text{ cm}^{-1}$ and $P' = 7.17 \times 10^{-6} \text{ cm}^{-1}$. Nuclear quadrupole moments in this region are of the order of 0.5 barns; thus P could be as high as $\sim 6 \times 10^{-6} \text{ cm}^{-1}$. Even so these theoretical estimates are much smaller than the experimental value for P" of $(7.3 \pm 0.4) \times 10^{-5} \text{ cm}^{-1}$.

The value of P' depends on the splitting between the lowest singlet and doublet. This splitting was theoretically investigated by varying the interpolated crystal field parameters and was found to be very sensitive to the values of $A_6^0 \langle r^6 \rangle$ and $A_6^6 \langle r^6 \rangle$. The size of the observed effect can easily be accounted for if the splitting is about 2 cm^{-1} instead of 19 cm^{-1} , and this splitting can easily be obtained by reducing $A_6^0 \langle r^6 \rangle$ and $A_6^6 \langle r^6 \rangle$. In fact one could infer from our experiment that $A_6^0 \langle r^6 \rangle$ is probably closer to -50 cm^{-1} than -40 cm^{-1} and that $A_6^6 \langle r^6 \rangle$ is somewhat lower than 700 cm^{-1} . It should be pointed out that adjusting the energy spacing

between the lowest singlet and doublet to fit the data is a valid procedure inasmuch as it requires changing $A_6^0\langle r^6 \rangle$ and $A_6^6\langle r^6 \rangle$ by amounts well within the accuracy to which they are known. The theoretical quadrupole coupling constant, P , is not appreciably altered by this procedure. It follows from this discussion that $P \leq 0.1P''$ for Pm^{144} ; i.e., that P'' is at least 90% pseudo-quadrupole. Thus it seems valid to derive, from the experimental μ and P'' of Pm^{144} , a spin-independent pseudo-quadrupole coupling constant C' . We shall account for the possibility of P'' for Pm^{144} being as much as 10% P in the limits of error for C' .

VI. NUCLEAR MOMENTS

Once it has been established that the pseudo-quadrupole mechanism is mainly responsible for producing the alignment of Pm^{+3} in CMN it becomes possible to derive nuclear moments for the various Pm isotopes. Shirley, et al.⁸ aligned Pm^{144} in NES and established that for $I = 5$, $|\mu| = 1.68 \pm 0.14$ n.m. and for $I = 6$, $|\mu| = 1.75 \pm 0.14$ n.m. From Table III we find $P'' = +(1.1 \pm 0.1) \times 10^{-4} \text{ cm}^{-1}$ for $I = 5$ and $P'' = +(7.3 \pm 0.4) \times 10^{-5} \text{ cm}^{-1}$ for $I = 6$. Using these values and Eq. 7 we can now calculate $C' = +(1.01 \pm 0.17) \times 10^{-3} \text{ cm}^{-1} (\text{n.m.})^{-2}$

A. Pm^{143}

The spin of Pm^{143} is almost certainly $5/2$ or $7/2$. For a spin of $7/2$ and the experimental $P'' = +(1.25 \pm 0.2) \times 10^{-3} \text{ cm}^{-1}$ we calculate the magnetic moment as $|\mu| = 3.9 \pm 0.5$ n.m., while for a spin of $5/2$ and the experimental $P'' = +(2.2 \pm 0.3) \times 10^{-3} \text{ cm}^{-1}$ we get a magnetic moment of $|\mu| = 3.75 \pm 0.5$ n.m. For an unpaired proton in a $g_{7/2}$ state the Schmidt and Dirac limits on the magnetic moment are 1.7 n.m. and 3.1 n.m. respectively. The Dirac and Schmidt limits for a proton in a $d_{5/2}$ state are 2.9 n.m. and 4.8 n.m. respectively. Since the value $|\mu| = 3.9 \pm 0.5$ n.m. falls outside the usual limits for a $g_{7/2}$ proton one could interpret this as weak evidence for the spin of Pm^{143} being $5/2$ rather than $7/2$.

B. (5.4 day) Pm^{148}

For (5.4 day) Pm^{148} we are able to combine the data shown in Figs. 9 and 10 to get the magnetic moment. Experimentally it is determined that U_2 must be negative for this transition (See Sec. III). Since only the $L=1 \beta$ transition produces a negative U_2 , one limit on U_2 must be for a pure $L=1 \beta$

decay, which has $U_2 = -0.50$. From the CMN data we can set the other limit on U_2 and we find $-0.50 < U_2 < -0.37$. Then using this value of U_2 in conjunction with the NES data in Fig. 10 we can set the limits on A ; $0.0316 \text{ cm}^{-1} < |A| < 0.0388 \text{ cm}^{-1}$. Now from the relation³⁴

$$|\mu| = \frac{|A| I}{0.0193} \quad (16)$$

We obtain $|\mu| = 1.82 \pm 0.19 \text{ n.m.}$

C. (41 day) Pm^{148}

The magnetic moment for (41 day) Pm^{148} is very simply evaluated from the NES data. Using the decay scheme (Fig. 8) modified by our results of Sec. III (i.e. that $I_{1.90} = I_{2.09} = I_{2.19} = 6+$ in Sm^{148} and that the spin of (41 day) Pm^{148} is 6-) we can set limits on U_2 of the 550 keV γ -ray; $0.52 < U_2 < 0.58$. From the data of Fig. 11 we then find $|A| = (5.8 \pm 0.6) \times 10^{-3} \text{ cm}^{-1}$ and using Eq. (16) the magnetic moment is evaluated as $|\mu| = 1.80 \pm 0.18 \text{ n.m.}$

D. Pm^{149}

Pm^{149} was aligned in CMN by Chapman et al.⁶ Since they did not have the value of C' in Eq. 7 they were unable to determine the magnetic moment of Pm^{149} . From their data we can obtain a value for P'' of $(8.8 \pm 2.1) \times 10^{-4} \text{ cm}^{-1}$ leading to a magnetic moment $|\mu| = 3.3 \pm 0.5 \text{ n.m.}$

VII. DISCUSSION

It is interesting to examine the magnetic moments for the spins 1 and 6 states of Pm^{148} . The shell model predicts the 61st proton of this odd-odd nucleus to have either a $d_{5/2}$ or $g_{7/2}$ configuration while the 87th neutron should have either an $f_{5/2}$ or $f_{7/2}$ configuration. There are seven ways in which to combine these states to make spins 1 and 6 and these possibilities are shown in Table V. Using the "Schmidt values" of the magnetic moments for unpaired protons and neutrons [μ ($d_{5/2}$ proton) = + 4.79 n.m., μ ($g_{7/2}$ proton) = + 1.72 n.m., μ ($f_{5/2}$ neutron) = + 1.37 n.m., and μ ($f_{7/2}$ neutron) = - 1.91 n.m.] and coupling the neutron and proton angular momenta, we obtain the values for the magnetic moments listed in column 4 of Table V. These values agree very poorly with the experimental values derived above. However since the Pm^{148} isomers are not near a closed shell for either protons or neutrons there is no a priori reason to expect these single-particle values to be applicable in this region.

Perhaps a more useful comparison with experiment can be provided by means of an empirical calculation³⁵ based on the ground-state spin assignments and magnetic moments of odd nucleons in neighboring nuclei. Table VI shows the values of μ which were used for the nominal $d_{5/2}$ and $g_{7/2}$ proton and $f_{5/2}$ and $f_{7/2}$ neutron configurations. Only the $d_{5/2}$ proton configuration value is rather arbitrary and this is not too important since both Pm^{147} and Pm^{149} have spins of 7/2, making it most likely that the 61st proton in Pm^{148} is in a 7/2+ configuration. The sign of μ for Nd^{147} was inferred from the Schmidt value. By coupling the g values shown in Table VI we calculated the empirical values of the magnetic moments shown in column 5 of Table V. Comparison of these values with the experimental results shows that good agreement is obtained if the ground state ($I = 1$) of

Pm^{148} is in a nominal $(g_{7/2} f_{5/2})$ configuration and the excited state ($I = 6$) has a nominal $(g_{7/2} f_{7/2})$ configuration. The coupling of spins in these configurations is contrary to Nordheim's rules but since we are dealing with multiple-particle configurations rather than single-particle configurations this disagreement may not be important.

VIII. ABSOLUTE TEMPERATURE SCALE FOR CMN

A careful inspection of Figure 2 will show that the axial data points, with the exception of the lowest temperature point, could be fitted slightly better by a curve with a small negative curvature in $I(\theta)$ vs T^{-1} indicating "saturation" of the nuclear alignment. Such a curve would be physically reasonable; it would correspond to a much larger value of P' than does the curve actually drawn in Fig. 2. If the lowest-temperature point were in reality at a much lower temperature still, it would lie on the "saturation" curve. If the $T-T^*$ relationship for CMN were considerably in error, the lowest temperature point could appear to be at too high a temperature. There is some evidence that the $T-T^*$ relationship for CMN might be in error in just this way, the lowest point lying at a temperature much lower than 0.003°K .^{38,39}

A more thorough analysis of the data in Fig. 2 tends to refute this interpretation for two reasons: (1) there is no detectable P_4 term in the angular distribution at the lowest temperature (Fig. 3), whereas the "saturation" curve would require the distribution $I(\theta) \approx 1 + 0.17 P_2(\cos \theta) - 0.03 P_4(\cos \theta)$ at this temperature; and (2) the magnitude of the limiting value for the coefficient of the P_2 term is $+ 0.40$ for this decay sequence; the saturation curve would require a value of $+ 0.18$

We conclude, then that the data for P_m ¹⁴⁴ qualitatively substantiate the magnetic temperature scale for CMN given by Daniels and Robinson.¹² It should be noted that this experiment is not highly sensitive to small inaccuracies in the $T-T^*$ scale, nor was the ultimate possible accuracy obtained. Still this measurement provides independent confirmation, by a unique method, that the $T-T^*$ relation for CMN is essentially correct.

REFERENCES

1. C. S. Wu, E. Ambler, R. W. Hayward, D. D. Hoppes, and R. P. Hudson, Phys. Rev. 105, 1413 (1957).
2. S. H. Hanauer, J. W. T. Dabbs, L. D. Roberts, and G. W. Parker, Phys. Rev. 124, 1512 (1961).
3. Grace, Johnson, Kurti, Scurlock, and Taylor, Conference de Physique des Basses Temperatures, 1955 (Centre National de la Recherche Scientifique and UNESCO, Paris, 1956).
4. B. N. Samoïlov, V. V. Sklvarevskii and E. P. Stepanov, Soviet Phys. JETP 36, 448 (1959).
5. B. R. Judd, C. A. Lovejoy and D. A. Shirley, Phys. Rev., to be published.
6. C. J. S. Chapman, M. A. Grace, J. M. Gregory and C. V. Sowter, Proc. Roy. Soc. A 259, 377 (1960).
7. C. A. Lovejoy, J. O. Rasmussen, and D. A. Shirley, Phys. Rev. 123, 954 (1961).
8. D. A. Shirley, J. F. Schooley and J. O. Rasmussen, Phys. Rev. 121, 558 (1961).
9. C. E. Johnson, J. F. Schooley, and D. A. Shirley, Phys. Rev. 120, 2108 (1960).
10. R. A. Erickson, L. D. Roberts and J. W. T. Dabbs, Rev. Sci. Instruments. 25, 1178 (1954).
11. H. Meyer, Phil. Mag. 2, 521 (1957).
12. J. M. Daniels and F. N. H. Robinson, Phil. Mag. 44, 630 (1953).
13. S. Ofer, Phys. Rev. 113, 895 (1959).
14. E. G. Funk Jr., J. W. Mihelich, and C. F. Schwerdtfeger, Phys. Rev. 120, 1781 (1960).

15. R. J. Blin-Stoyle and M. A. Grace, Handbuch der Physik, Vol. 42, P. 555.
16. A. R. Edmonds, Angular Momentum in Quantum Mechanics (Princeton, 1957), page 97.
17. J. Weneser and D. R. Hamilton, Phys. Rev. 92, 321 (1953).
18. N. Starfelt and J. Cederlund, Phys. Rev. 105, 241 (1957).
19. M. Murakawa and J. S. Ross, Phys. Rev. 82, 967 (1951).
20. B. Budick, W. M. Doyle, R. Marrus, and W. A. Nierenberg, Bull. Am. Phys. Soc. Ser. II, Vol. 7, pp. 476.
21. G. A. Westenbarger and D. A. Shirley, Phys. Rev. 123, 1812 (1961).
22. S. K. Bhattacharjee, B. Sahai and C. V. K. Baba, Nuclear Phys. 12, 356 (1959).
23. C. F. Schwerdtfeger, E. G. Funk Jr., and J. W. Mihelich, Phys. Rev. 125, 1641 (1962).
24. C. W. Reich, R. P. Schuman, J. R. Berreth, M. K. Brice and R. L. Heath, Phys. Rev. 127, 192 (1962).
25. T. Lindquist and E. Heer (note added in proof, quoting communications from M. A. Grace), Nuclear Phys. 2, 686 (1957).
26. S. Ofer, Phys. Rev. 114, 870 (1959).
27. C. H. Townes, Handbuch der Physik, Vol. 38/1, pp. 402.
28. R. J. Elliott and K. W. H. Stevens, Proc. Roy. Soc. A 219, 387 (1953).
29. B. R. Judd, Proc. Roy. Soc. A 232, 462 (1955).
30. R. J. Elliott, Proc. Phys. Soc. B 70, 119 (1957).
31. B. R. Judd and I. Lindgren, Phys. Rev. 122, 1802 (1961).
32. E. C. Ridley, Proc. Camb. Phil. Soc. 56, 41 (1960).
33. M. H. Crozier and W. A. Runciman, J. Chem. Phys. 35, 1392 (1961).
34. H. J. Stapelton, C. D. Jeffries and D. A. Shirley, Phys. Rev. 124, 1455 (1961).

35. C. A. Lovejoy and D. A. Shirley Nuclear Phys. 30, 452 (1962).
36. I. Lindgren, Nuclear Phys. 32, 151 (1962).
37. K. Murakawa, J. Phys. Soc. Japan 15, 2306 (1960).
38. R. P. Hudson, R. S. Kalser, and H. E. Radford, Proceedings of the VII International Conference on Low Temperature Physics, p. 100 (University of Toronto Press, 1961).
39. D. de Klerk, Handbuch der Physik (Berlin: Springer, 1956) Vol. XV, 118.

Table I

E_{γ} keV	I(0)
474	1.106 ± 0.008
615	1.141 ± 0.008
695	1.137 ± 0.008

I(0) for the 474, 615 and 695 keV
 γ -rays observed in the decay of
 ^{144}Pm aligned in CMN at 0.0031°K .

Table II

E_{γ} keV	I(0)
550	0.920 ± 0.006
627	0.910 ± 0.006
723	0.919 ± 0.008
913	0.908 ± 0.010
1011	0.902 ± 0.008

Intensities for γ -transitions observed
in the decay of aligned (41 day) Pm^{148}
along the crystalline C axis and at
 $T = 0.02^{\circ}\text{K}$. in NES.

Table III

Isotope	I-spin	$ A (10^{-3} \text{ cm}^{-1})$	$P'' (10^{-3} \text{ cm}^{-1})$
Pm^{143}	5/2	29 (3)	2.2 (.3)
	7/2	22 (2)	1.25 (.20)
Pm^{144}	5	6.5 (.5)	0.11 (.01)
	6	5.6 (.5)	0.073 (.004)
(5.4 day) Pm^{148}	1	35 (4)	3.3 (.7)
(41 day) Pm^{148}	6	5.8 (.3)	_____
Pm^{149}	7/2	_____	0.88 (.2)

Hyperfine structure coupling constants, A , and total quadrupole coupling constants, P'' , for several Pm isotopes in NES and CMN, respectively. Errors are given parenthetically.

Table IV

Energies (cm^{-1})	Degeneracy	Wave functions in $ J_z\rangle$ notation
-181.66	1	$+0.56 +3\rangle + 0.61 0\rangle - 0.56 -3\rangle$
-162.82	2	$+0.66 \pm 4\rangle \mp 0.73 \pm 1\rangle + 0.21 \mp 2\rangle$
-123.51	2	$\pm 0.475 \pm 4\rangle + 0.18 \pm 1\rangle \mp 0.86 \mp 2\rangle$
172.53	1	$+0.71 +3\rangle + 0.71 -3\rangle$
193.91	2	$+0.59 \pm 4\rangle \pm 0.66 \pm 1\rangle + 0.46 \mp 2\rangle$
194.00	1	$-0.43 +3\rangle + 0.79 0\rangle + 0.43 -3\rangle$

Energies and wave functions of the eigenstates of 5I_4 Pm^{+3} in CMN, calculated from crystal field theory with parameters given in text.

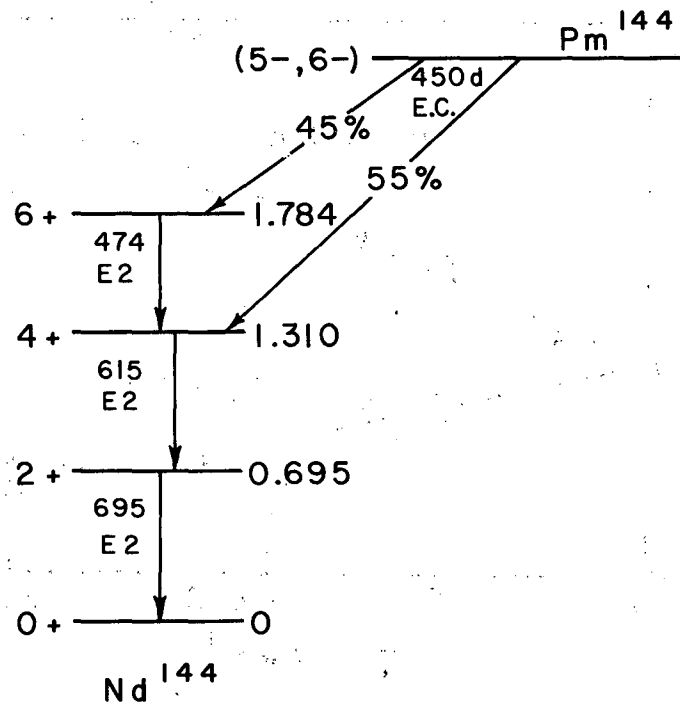
Table V

Proton con- figuration	Neutron con- figuration	I	μ (n.m.) Schmidt value	μ (n.m.) Empirical value	Agreement with Nordheim's rules
$d_{5/2}$	$f_{7/2}$	1	-3.62	-2.80	No
$d_{5/2}$	$f_{7/2}$	6	2.88	3.65	Yes
$d_{5/2}$	$f_{5/2}$	1	1.23	1.01	Yes
$g_{7/2}$	$f_{7/2}$	1	-0.03	0.31	Yes
$g_{7/2}$	$f_{7/2}$	6	-0.18	1.84	No
$g_{7/2}$	$f_{5/2}$	1	0.42	1.67	No
$g_{7/2}$	$f_{5/2}$	6	3.09	3.52	Yes

Possible proton and neutron configurations which would give spins 1 and 6 for Pm^{148} . Agreement with the experimental values of $|\mu| = 1.8$ for both states is obtained for the configurations $(g_{7/2}f_{7/2})$ and $(g_{7/2}f_{5/2})$.

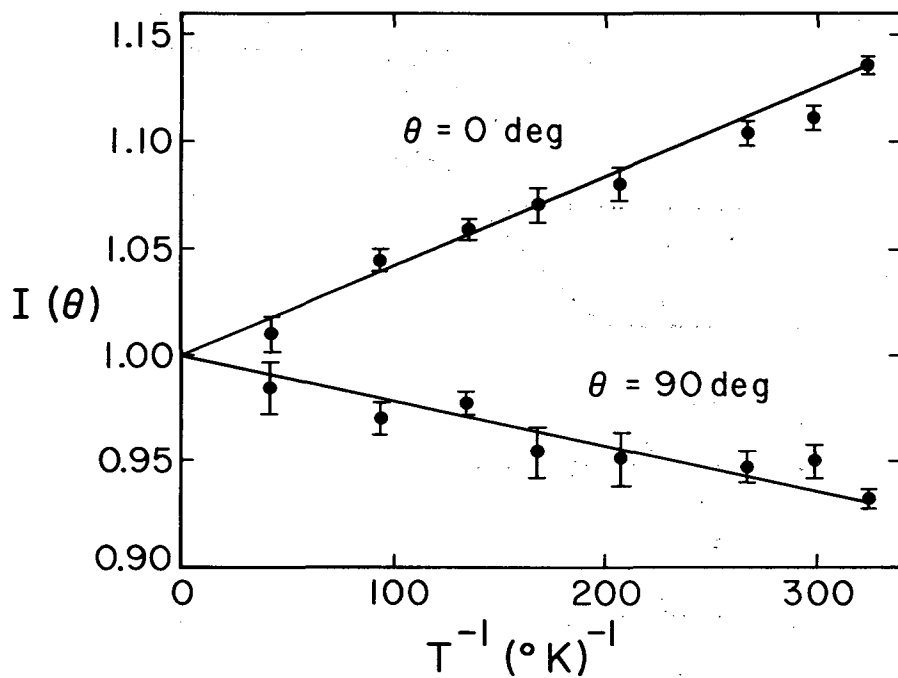
Table VI

Odd-A nucleus	Ground-state spin (I)	Nominal configuration	μ (n.m.)	g (n.m.)	ref.
${}_{61}^{\text{Pm}}{}^{147}_{86}$	7/2	$g_{7/2}$	(+) 3.0	(+) 0.86	34
${}_{60}^{\text{Nd}}{}^{147}_{87}$	5/2	$f_{5/2}$	(+) 0.53	(+) 0.21	36
${}_{62}^{\text{Sm}}{}^{149}_{87}$	7/2	$f_{7/2}$	- 0.85	- 0.24	36
${}_{59}^{\text{Pr}}{}^{141}_{82}$	5/2	$d_{5/2}$	+ 4.0		37
			+ 5.1		36
			+ 4.8	+ 1.80	Schmidt value
			+ 4.5		Value used
Nuclear moments of odd-A nuclei in the neighborhood of ${}_{61}^{\text{Pm}}{}^{148}$					



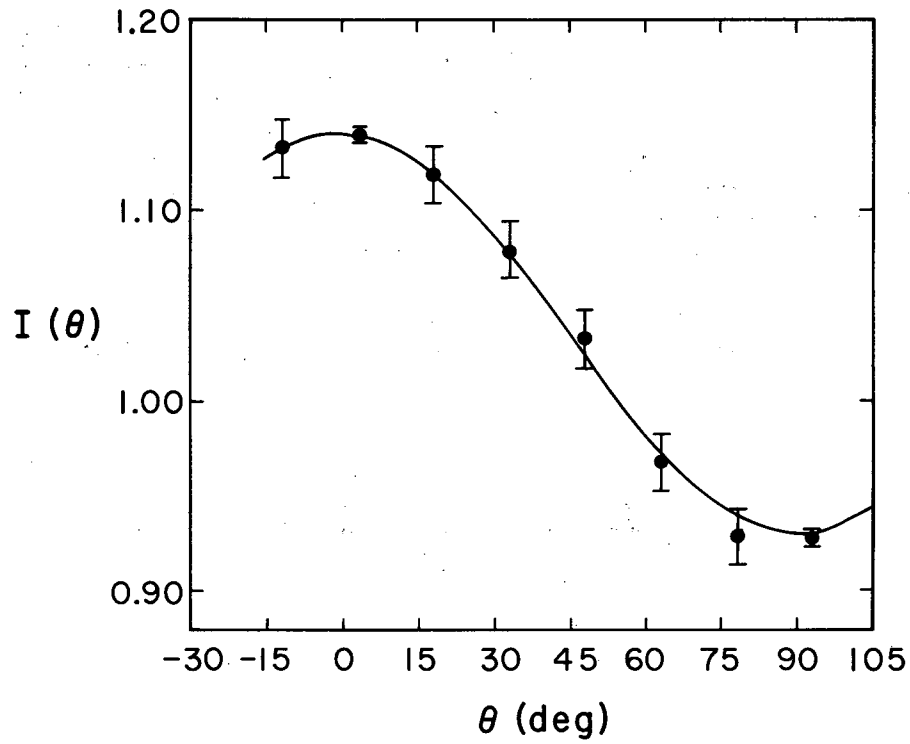
MU-28202

Fig. 1. Decay scheme of Pm^{144} after Ofer. 13



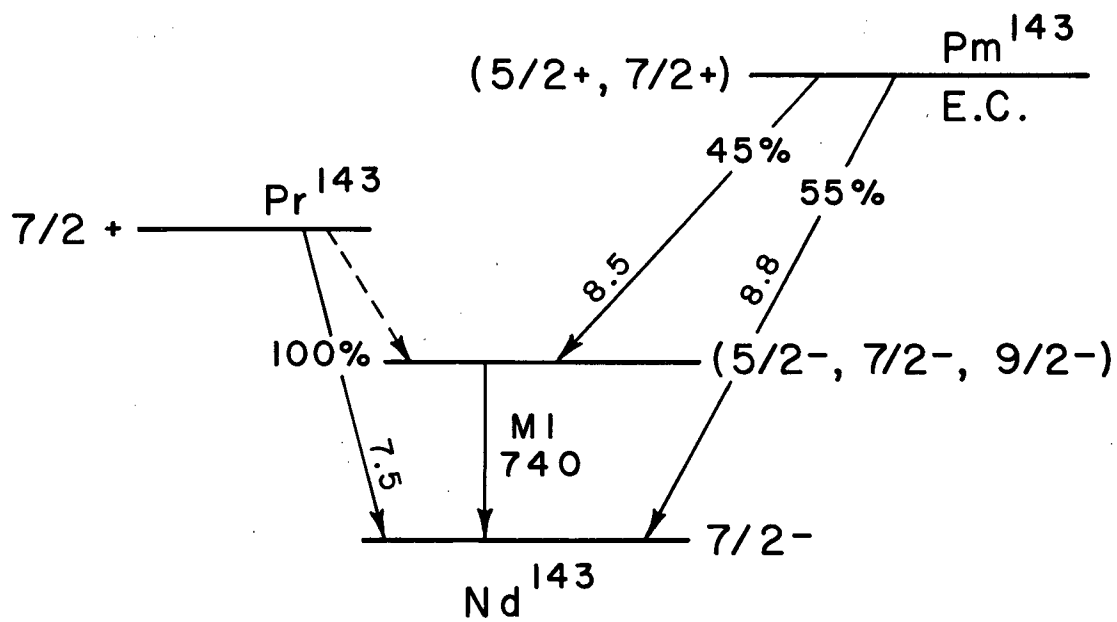
MU-28203

Fig. 2. Temperature dependence of $I(\theta)$ for the 695 keV γ -ray in the decay of aligned Pm^{144} taken at 0° and 90° from the crystalline C axis in CMN. Normalized theoretical curves were calculated from Eqs. (2) and (5).



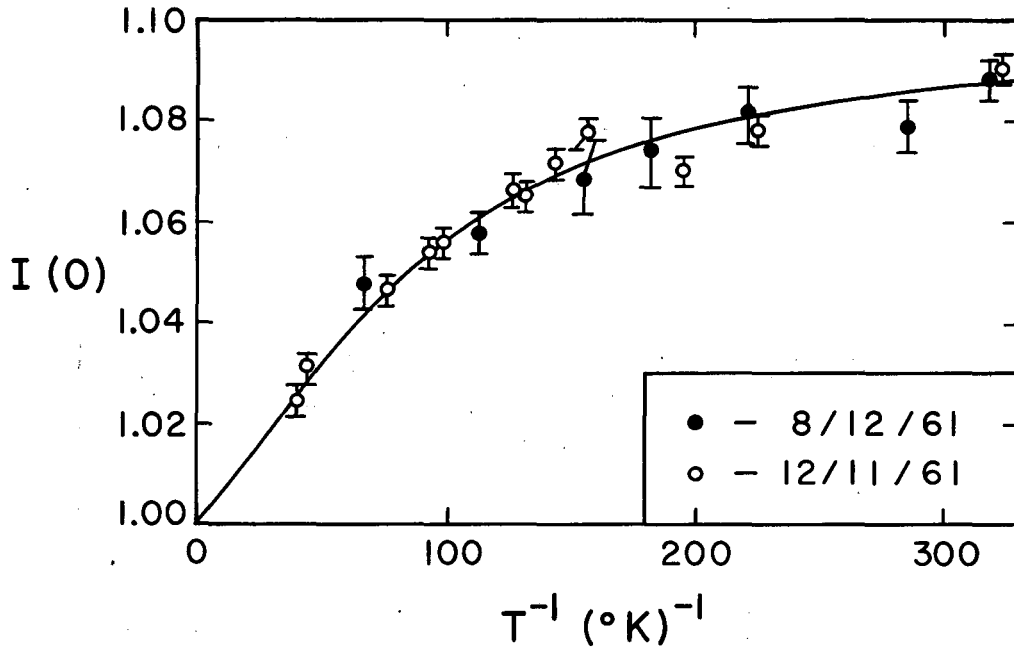
MU-28204

Fig. 3. Intensity vs. angle from the C axis, θ , for the 615 keV γ -ray in the decay of Pm^{144} . The data were taken at $T = 0.0031^\circ \text{K}$ in CMN. The solid curve is $1 + 0.14 P_2(\cos \theta)$.



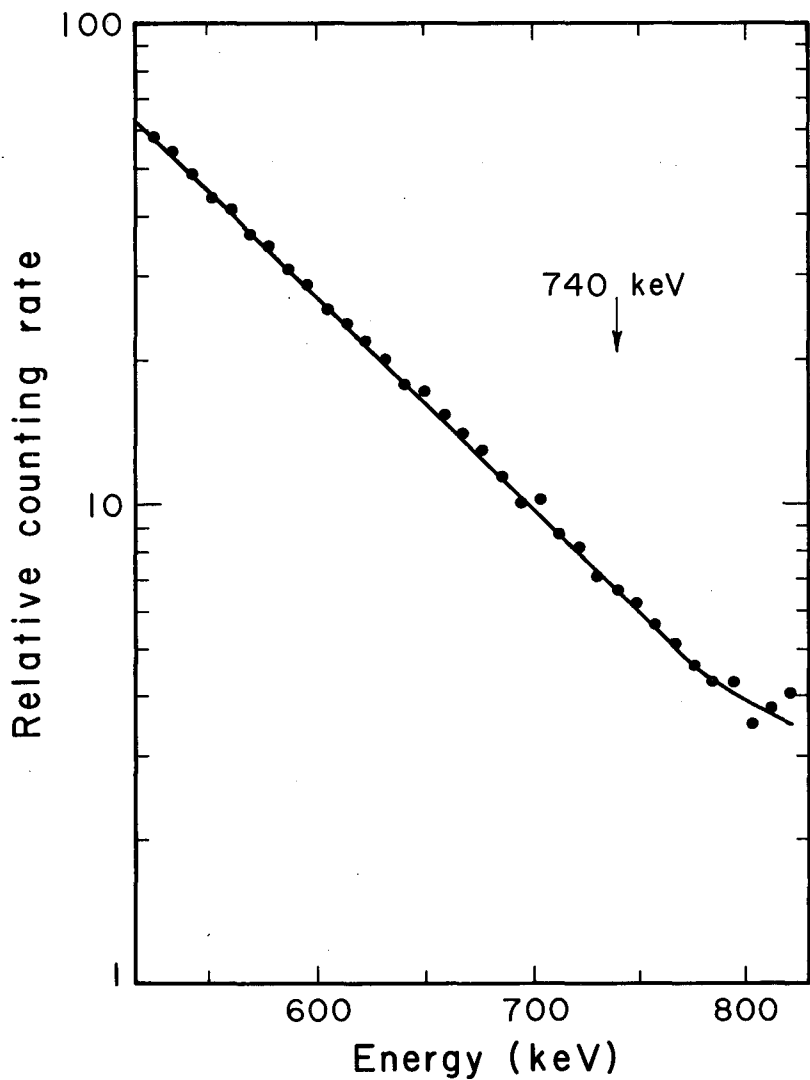
MU-28205

Fig. 4. Decay schemes of Pm^{143} and Pr^{143} .



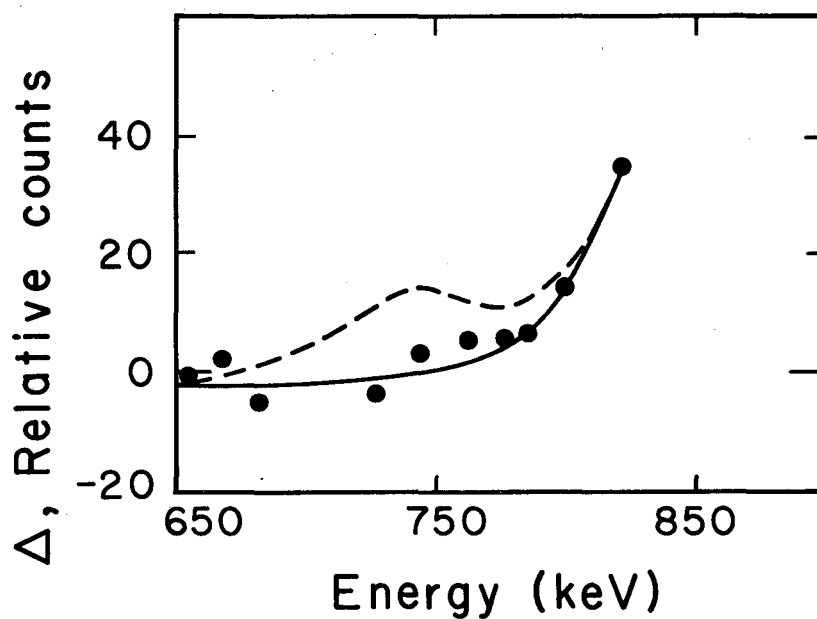
MU-28206

Fig. 5. Temperature dependence of $I(0)$ for the 740 keV γ -ray in the decay of Pm^{145} in CMN. Data of August 12, 1961 and December 11, 1961 are shown with normalized theoretical curve calculated by using Eqs. (2) and (5).



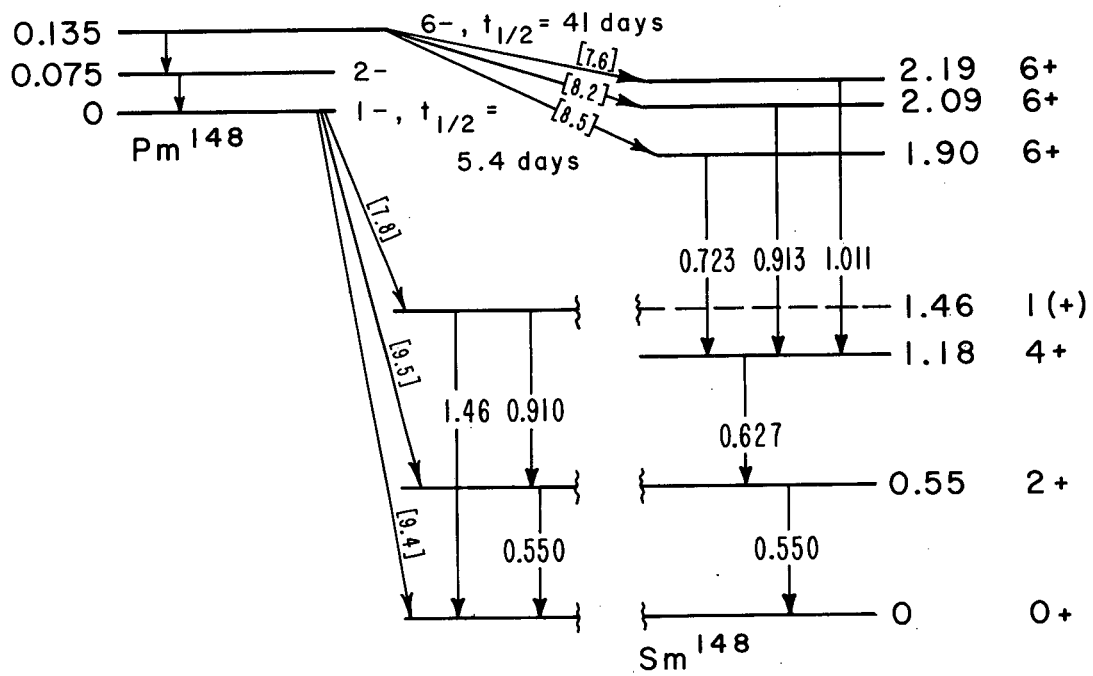
MU-28207

Fig. 6. Scintillation spectrum observed in decay of Pr¹⁴³ plotted on a semi-log scale so that background due to bremsstrahlung will be linear.



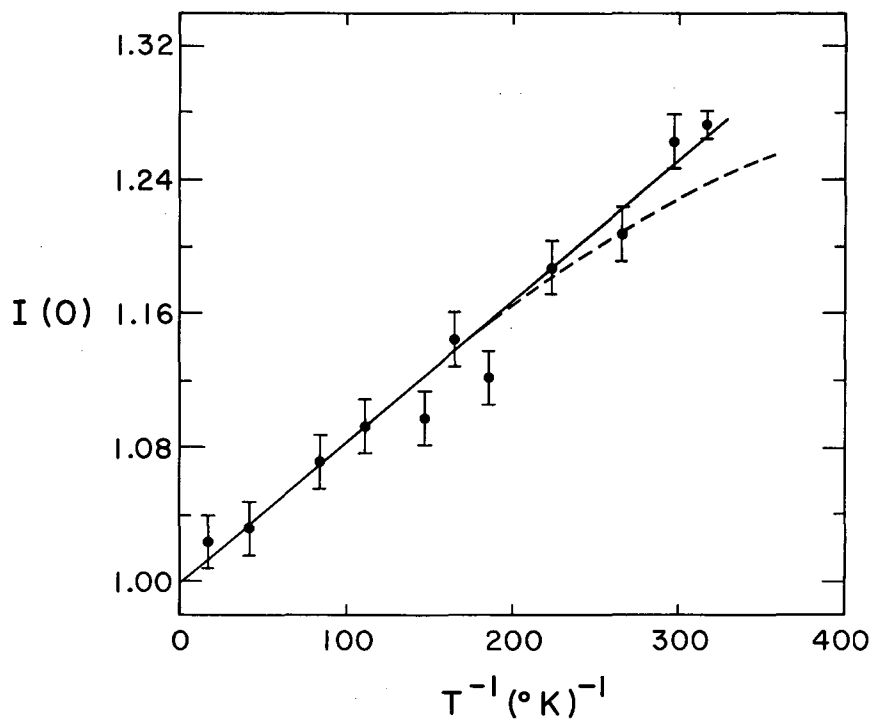
MU-28208

Fig. 7. The difference plot of Δ (defined in text) vs. energy. Dashed curve would be expected if $1.5 \times 10^{-4}\%$ of decays produced 740 keV γ -rays.



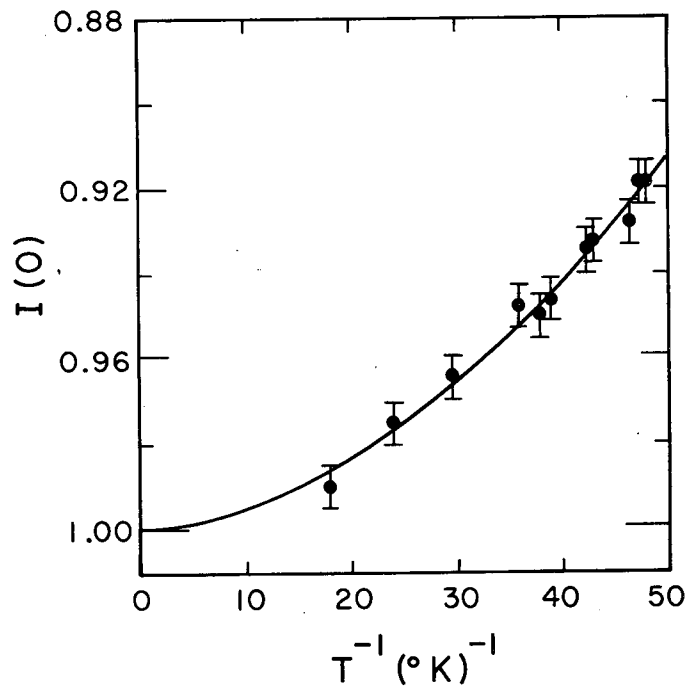
MU-28209

Fig. 8. Decay scheme of the Pm^{148} isomers relevant to our research as given in ref. 24 and modified by this work.



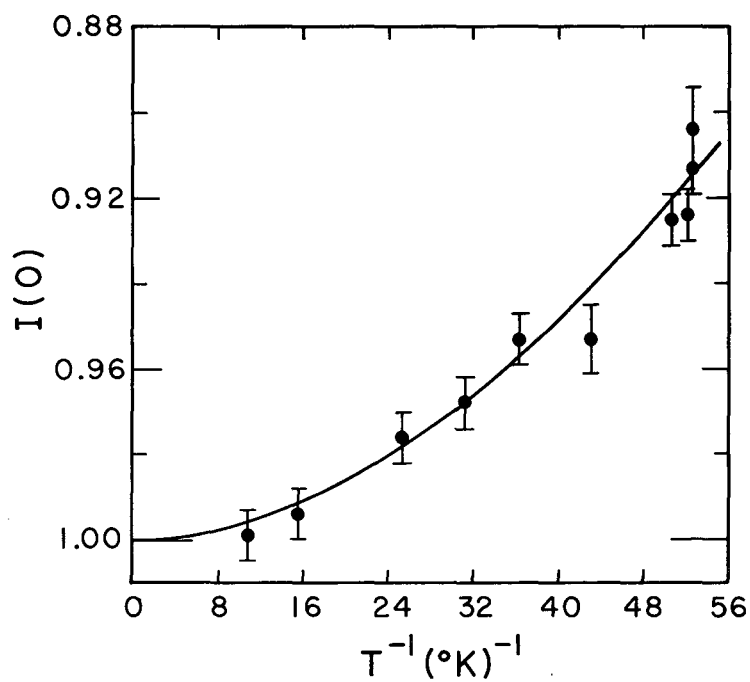
MU-28210

Fig. 9. Temperature dependence of $I(0)$ for the 1460 keV γ -ray in the decay of (5.4 day) Pm^{148} in CMN. Data are shown with normalized theoretical curve calculated from Eqs. (2) and (5). For explanation of dashed curve see Sec. III C.



MU-28211

Fig. 10. Temperature dependence of $I(0)$ for the 1460 keV γ -ray in the decay of aligned (5.4 day) Pm^{148} in NES. Data are shown with normalized theoretical curve calculated by using Eqs. (2) and (4).



MU-28212

Fig. 11. Temperature dependence of $I(0)$ for the 550 keV γ -ray in the decay of aligned (41 day) Pm^{148} in NES. Data are shown with normalized theoretical curve calculated by using Eqs. (2) and (4).

This report was prepared as an account of Government sponsored work. Neither the United States, nor the Commission, nor any person acting on behalf of the Commission:

- A. Makes any warranty or representation, expressed or implied, with respect to the accuracy, completeness, or usefulness of the information contained in this report, or that the use of any information, apparatus, method, or process disclosed in this report may not infringe privately owned rights; or
- B. Assumes any liabilities with respect to the use of, or for damages resulting from the use of any information, apparatus, method, or process disclosed in this report.

As used in the above, "person acting on behalf of the Commission" includes any employee or contractor of the Commission, or employee of such contractor, to the extent that such employee or contractor of the Commission, or employee of such contractor prepares, disseminates, or provides access to, any information pursuant to his employment or contract with the Commission, or his employment with such contractor.

